Mechanism of and exquisite selectivity for O–O bond formation by the heme-dependent chlorite dismutase

Amanda Q. Lee*, Bennett R. Streit†, Michael J. Zdilla*, Mahdi M. Abu-Omar*‡, and Jennifer L. DuBois†‡

*Brown Laboratory, Department of Chemistry, Purdue University, 560 Oval Drive, West Lafayette, IN 47907; and †Department of Chemistry and Biochemistry, University of Notre Dame, Notre Dame, IN 46556

Edited by Harry B. Gray, California Institute of Technology, Pasadena, CA, and approved August 15, 2008 (received for review May 2, 2008)

Chlorite dismutase (Cld) is a heme b-dependent, O–O bond forming enzyme that transforms toxic chlorite (ClO_2^-) into innocuous chloride and molecular oxygen. The mechanism and specificity of the reaction with chlorite and alternate oxidants were investigated. Chlorite is the sole source of dioxygen as determined by oxygen-18 labeling studies. Based on ion chromatography and mass spectrometry results, Cld is highly specific for the dismutation of chlorite to chloride and dioxygen with no other side products. Cld does not use chlorite as an oxidant for oxygen atom transfer and halogenation reactions (using cosubstrates guaiacol, thioanisole, and monochlorodimedone, respectively). When peracetic acid or H_2O_2 was used as an alternative oxidant, oxidation and oxygen atom transfer but not halogenation reactions occurred. Monitoring the reaction of Cld with peracetic acid by rapid-mixing UV-visible spectroscopy, the formation of the high valent compound I intermediate, [(Por$^{\bullet+}$)Fe^{IV} = O], was observed [$k_1 = (1.28 \pm 0.04) \times 10^6$ M^{-1} s^{-1}]. Compound I readily decayed to form compound II in a manner that is independent of peracetic acid concentration (k_2 = 170 ± 20 s^{-1}). Both compound I and a compound II-associated tryptophanyl radical that resembles cytochrome c peroxidase (Ccp) compound I were observed by EPR under freeze-quench conditions. The data collectively suggest an O–O bond-forming mechanism involving generation of a compound I intermediate via oxygen atom transfer from chlorite, and subsequent recombination of the resulting hypochlorite and compound I.

dioxygen | compound I | peroxidase | peroxygenase | chlorite

Nature makes use of heme iron for a range of oxidation, reduction, atom transfer, electron transfer, and small-molecule sensing and trafficking processes, with a specificity that is sometimes difficult or impossible to reproduce synthetically. The catalytic flexibility of the heme/protein combination is especially valuable for the evolution of new catalytic activities in response to environmental change.

Chlorite dismutase (Cld) is a heme b-dependent enzyme that transforms ClO_2^- to Cl^- and O_2. The presence of its encoding gene is the hallmark of bacterial perchlorate (ClO_4^-) or chlorate (ClO_3^-) respiratory pathways (1). The existence of these pathways is remarkable, because perchlorate is primarily an anthropogenic substance that has only recently entered the environment in large amounts (2). The bacteria reduce perchlorate to chlorate and chlorate to chlorite via a molybdopterin-dependent perchlorate reductase (PerR), a close homolog of bacterial respiratory nitrate reductases. By contrast, chlorite dismutase has no sequence homologs in the existing databases (2). Its role is to detoxify chlorite, a by-product of perchlorate or chlorate respiration. As such, it also has no functional correlate in the nitrate respiratory pathways, which reduce NO_3^- completely to NH_3 or N_2 (3).

The potential bioremediation of toxic oxochlorate contamination in soil and ground water has motivated study of the biology of perchlorate-respiring bacteria, PerR, and Cld (4). At the same time, mechanisms of O–O bond formation are of intense interest to inorganic chemists aiming to catalyze water oxidation or to understand the fundamental reactivity of metal-oxo species in dioxygen production (5, 6) and oxidation chemistry (7). Cld, a simple heme/protein system, is the only enzyme other than photosystem II to catalyze O–O bond formation as its primary function. We were therefore interested, first, in probing whether O_2 evolution by Cld occurs through a peroxidase-like iron-oxo intermediate and, second, in determining how specific Cld is for this reaction.

Heme enzymes react with chlorite, a strong oxidant, in a variety of ways. Heme peroxidases use chlorite as an oxidant in one-electron oxidation (8), oxygen atom transfer (OAT) (9), and chlorination chemistry (10, 11). Ferric horseradish peroxidase (HRP) and cytochrome P450 react with chlorite to generate the reactive ferryl porphyrin cation radical (compound I) intermediate (8, 11). Cld could potentially use chlorite in any of these types of reactions. Further, although Cld does not share sequence homology with canonical heme peroxidases, their active sites contain the same histidine-ligated heme b as the catalytic moiety (12). In the presence of chlorite, peroxide (H_2O_2), or peracids (ROOH), it is possible that Cld could form peroxidase-like reactive intermediates that would potentially be available for oxidation chemistry. Herein, we show that Cld is extraordinarily specific for the conversion of its native substrate ClO_2^- to Cl^- to O_2, with no observed side reactions. We also define the scope of observed reactivities of Cld with other oxidants, determine the origin of the dioxygen product via ^{18}O-labeling studies, and characterize high-valent oxo intermediates and their stopped-flow kinetics. These studies support a proposed mechanism for chlorite dismutation and demonstrate the acuity with which this enzyme is adapted for its native reaction.

Results

Reaction of Cld and Chlorite: Oxygen-18 Labeling Studies. When chlorite dismutation was carried out in isotope oxygen-18–enriched water (95%), a mass peak of m/z = 32 (^{16}O–^{16}O) with no traces of masses 34 (^{16}O–^{18}O) or 36 (^{18}O–^{18}O) was exclusively detected. Identical results were obtained when normal abundance isotope oxygen-16 water was used. All other peaks in the mass spectrum besides oxygen were detected in controls lacking the enzyme and attributed to the carrier gas (N_2) and impurities (H_2 and H_2O) in the carrier gas (Fig. 1). When dismutation of $Cl^{18}O_2^-$ was carried out in unlabeled aqueous buffer, a mass peak of 36 (^{18}O–^{18}O) was dominant, with smaller 34 and 32 peaks, consistent with the incomplete (77%) enrichment of the original $NaCl^{18}O_2$ sample (Fig. 1). These results indicate that both oxygen atoms in the evolved O_2 derive from chlorite, and that

Author contributions: M.M.A.-O. and J.L.D. designed research; A.Q.L., B.R.S., and M.J.Z. performed research; M.M.A.-O. and J.L.D. analyzed data; and M.M.A.-O. and J.L.D. wrote the paper.

The authors declare no conflict of interest.

This article is a PNAS Direct Submission.

‡To whom correspondence may be addressed. E-mail: mabuomar@purdue.edu or jdubois@nd.edu.

This article contains supporting information online at www.pnas.org/cgi/content/full/0804279105/DCSupplemental.

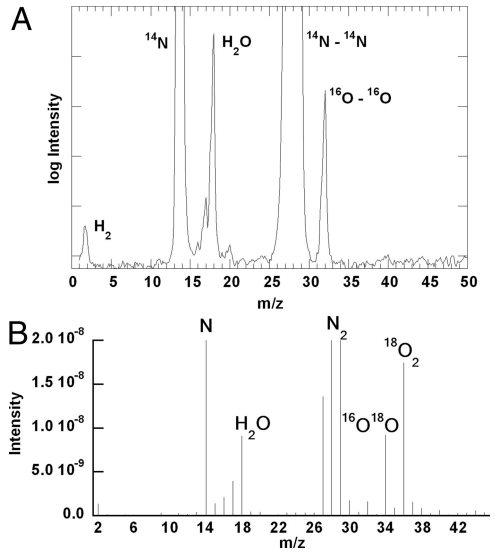

Fig. 1. Mass spectrum of gaseous products from the reaction of 85 nM Cld with 50 mM chlorite in 0.1 M sodium phosphate buffer, pH 7, made in 95% oxygen-18 enriched water (*A*) and by using enriched 18-O chlorite in $^{16}OH_2$ (*B*). Signal assignments (*m/z*): H_2 (2), N (14), H_2O (18), N_2 (28), $^{16}O_2$ (32), $^{18}O_2$ (36).

oxygen atom exchange between solvent water and potential reactive intermediates is insignificant.

Reaction of Cld and Chlorite: Quantitation of Cld Dismutation Products. The ion chromatogram of Cld dismutation products [supporting information (SI) Fig. S1] shows the only ionic and chlorine-containing species detected from the enzymatic reaction are chloride (49%) and unreacted chlorite (51%). As previously described, the enzyme deactivates under these conditions before all of the chlorite substrate is consumed (12). The yield of dioxygen (41%) determined by volumetric displacement is consistent with that of chloride, demonstrating a stoichiometry of 1:1 for O_2:Cl^-. A small amount of chlorate is detected by IC. However, this is present in the starting chlorite and it does not change beyond experimental uncertainty during the course of the reaction (Table S1). These results are consistent with oxygen electrode and iodometric titration methods (12).

Reactions of Cld and Chlorite in the Presence of Oxidation and Halogenation Cosubstrates. Guaiacol, thioanisole, and monochlorodimedone (MCD) were chosen as a nearly isosteric set of substrates diagnostic for peroxidase (1e$^-$ oxidation), peroxygenase (OAT), and halogenation reactivity. Because the pK_a for chlorous acid ($HClO_2$) is 1.72 and the reactive state ($HClO_2$ or ClO_2^-) of the substrate is unknown, reactions were examined at neutral (6.8) and low (4) pH (12). Lower pH values were inaccessible because of enzyme instability. No pH dependence was observed.

Incubating Cld with excess guaiacol or 2,2′-azino-bis(3-ethylbenzthiazoline-6-sulfonic acid) (ABTS) under turnover conditions (20,000 eq chlorite) led to no appreciable observed 1e$^-$ oxidized product. Similarly, under turnover conditions with chlorite in the presence of excess thioanisole, Cld does not generate an appreciable amount of the corresponding sulfoxide. Even with 1,250 eq thioanisole per heme, a conversion rate of only 0.0015 oxidized product:thioanisole was observed. This was only slightly above control reactions containing either no enzyme or 1 μM $FeCl_3$ ($\leq$0.00080 product:thioanisole) (Table S2 and Fig. S2).

Finally, Cld was screened for its ability to use chlorite to halogenate MCD. Like HRP, Cld could oxidize chlorite by one electron to generate chlorine dioxide (ClO_2), which readily chlorinates MCD in an uncatalyzed fashion (8). Or, Cld could react with chlorite to generate compound I (see below), which could oxygenate halide ions, if present. Many peroxidases oxidize Br^- or I^- to their corresponding hypohalides, which react spontaneously with MCD. Chloroperoxidase (CPO) and myeloperoxidase additionally oxidize Cl^- (13). HRP oxidizes Cl^- under some conditions, the resulting OCl^-/HOCl functionalizing the heme's vinyl substituents and inactivating the enzyme (14). Last, Cld could use chlorite to generate ClO^-/HClO ($pK_a \approx 7.5$). With HRP, transfer of an oxygen atom from $HClO_2$ to the ferric heme yields compound I and HClO. Free HClO readily chlorinates MCD.

In the presence of a large excess of chlorite and 100 μM MCD, conditions resulting in stoichiometric chlorination (via ClO_2) by HRP (8), no Cld-mediated chlorination is observed. Under the same conditions and with a halogen anion (Cl^-, Br^-, I^-) in excess, no halogenation was observed.

Reaction of Cld and Peracetic Acid. Cld rapidly forms a species with the characteristic compound II ($Fe^{IV}(O)$(por)) UV-visible (UV-vis) spectrum on treatment with $\geq$2 eq of peroxyacetic acid (PAA) or hypochlorite. More than 200 eq results in bleaching of the heme absorption with no detectable buildup of other species (12). Titration of Cld with PAA, peroxide, *meta*-chloroperbenzoic acid (*m*CPBA), or ClO^- resulted in gradual bleaching of the heme spectrum. PAA and peroxide show nearly complete bleaching after the addition of 100 eq (relative to heme), whereas *m*CPBA and ClO^- required $\approx$80 eq (Fig. S3). It was previously shown that $\approx 2.0 \times 10^4$ eq ClO_2^- are necessary for bleaching the chromophore, because the majority of the chlorite is converted to Cl^- and O_2 (12).

Reactions of Cld and Peracetic Acid in the Presence of Oxidation and Halogenation Cosubstrates. Incubation of Cld in the presence of the peroxidase substrates guaiacol or ABTS resulted in catalytic 1e$^-$ oxidations when PAA (1–5 eq) was used as the oxidant. Approximately 1.6 eq of ABTS radical were formed per mol of PAA consumed. This indicates that both oxidizing equivalents of PAA are used in catalyzing 1e$^-$ oxidations. The discrepancy from the expected 2:1 stoichiometry may be due to PAA-dependent heme decomposition (see Fig. S3). Cld transformed successive additions of guaiacol, indicating that the reaction is catalytic. Thioanisole was oxidized to the corresponding sulfoxide, although substoichiometrically (0.247 $\pm$ 0.003 eq of sulfoxide per PAA). PAA reacts directly with Br^- or I^- in aqueous solution; H_2O_2 was used as an oxidant with these anions. No halogenation in the presence of PAA/Cl^- or H_2O_2 and excess Cl^-, Br^-, or I^- was observed.

Reaction of Cld and Peracetic Acid: Detection of High-Valent Ferryl Intermediates. Compounds I and II have distinct UV-vis features. In general, the Soret absorbance (for HRP, λ_{max} = 402 nm, ε = 102 mM^{-1} cm^{-1}) diminishes in intensity by approximately half and shifts slightly in energy on formation of compound I (λ_{max} = 400 nm, ε = 53.8 mM^{-1} cm^{-1}, HRP). Reduction of compound I by one electron yields compound II, which has a strongly red-shifted Soret band with an absorptivity similar to that of the starting ferric form (λ_{max} = 420 nm, ε = 105 mM^{-1} cm^{-1}, HRP). The visible α, β, and charge transfer (CT) bands, although far less intense than the Soret, also undergo shifts. The ferric HRP spectrum is characterized by two-prominent CT bands at 498 and 643 nm and very weak α- and β-bands (580, 530 nm). These become prominent α- and CT-bands at 577 and 651 nm, with β appearing as a shoulder at 525 nm for compound I. Compound II has α- and β-bands forming a two-peaked spectrum with λ_{max} 555 and 527 nm (13) (Table S3).

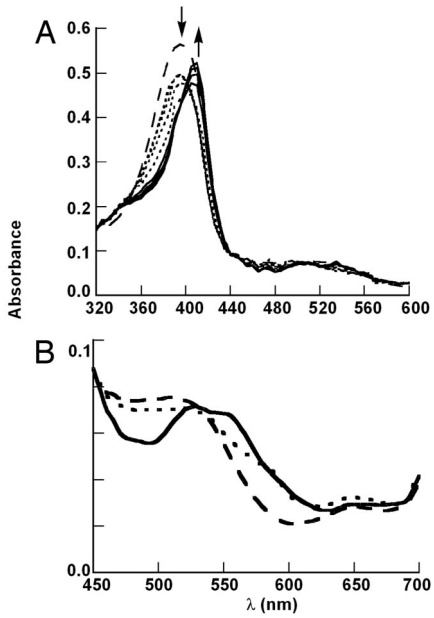

Fig. 2. Spectral changes within the first 20 ms after 10 μM Cld was mixed with 20 eq of PAA. Dashed line, ferric enzyme; dotted lines, compound I; solid lines, compound II. (*A*) Complete spectrum. (*B*) Visible region on an expanded scale.

Cld compound I can be detected by stopped-flow UV-vis spectroscopy after reaction with 20 eq of PAA at 10°C, as characterized by a decrease in the Soret band intensity (≈20% hypochromicity) with isobestic points at 355 nm and 440 nm (Fig. 2*A*). Within 20 ms, compound I decays to compound II (≈100% yield with respect to the starting enzyme concentration) as the Soret red-shifts to 415 nm, accompanied by an increase in the Soret absorbance. Changes in the visible bands reminiscent of HRP in the ferric, compound I, and compound II forms described above are also observed (Fig. 2*B*). Prominent peaks at ≈520 and 650 nm are likely CT bands, with much weaker α- and β-bands in between. These become a broad peak near 585 nm and a CT near 650 nm for compound I, and a clear double-peaked spectrum with maxima at ≈526 and 555 nm for compound II. Under these conditions, compound II is stable for >10 s before bleaching is detectable.

When one- or two-electron reductants are added in sequential mixing stopped-flow experiments, the spectral intermediates revert to the ferric starting spectrum. From the data in Fig. 2, it was determined that delay times of 10 and 20 ms after mixing the ferric enzyme with PAA were optimal for forming compound I or compound II, respectively. The ferric enzyme is regenerated from compound II by adding ≈600 eq of ascorbate ($1e^-$ reductant) 20 ms after mixing Cld and PAA in the stopped flow. An increase in absorbance at 395 nm (ferric enzyme) coincides with decrease of compound II at 415 nm. Compound I is also converted back to ferric Cld by the $2e^-$ electron reductant and oxygen atom acceptor thioanisole (Fig. S4). Addition of 1,500 eq of thioanisole 10 ms after mixing ferric Cld and PAA results in an increase in the 395-nm absorption band of the ferric form of the enzyme. The recovery of Fe(III) from compound I was not quantitative because the bimolecular reaction of compound I with thioanisole competes with compound I's rapid unimolecular conversion to compound II (see *Kinetics of Compounds I and II Formation*). Hence, the resulting spectrum is most consistent with the recovery of (approximately) 27% ferric enzyme, 63% conversion to compound II, and 10% signal bleaching.

When 20 eq of ClO^- were reacted with Cld, we did not observe a distinct compound I spectrum by stopped-flow techniques

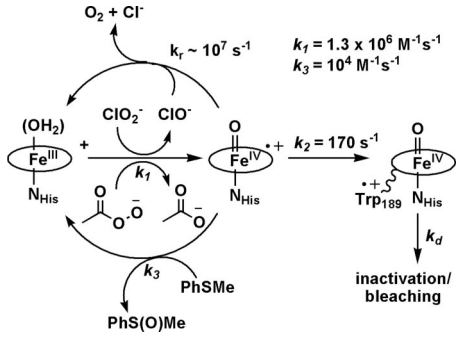

Scheme 1

(Fig. S5). Hypochromicity of the Soret occurred until ≈1 s, accompanied by a slight shift of the Soret, α- and β-bands from 410, 530, and 570 nm, respectively, to eventually a distinct compound II spectrum (413, 525, and 555 nm), which persists for at least 50 s before bleaching is detectable.

Kinetics of Compounds I and II Formation. Absorption spectroscopy suggests the formation of compound I from PAA followed by compound II formation:

$$\mathrm{Fe(III)(Por)} + \mathrm{CH_3COOO^-} \xrightarrow{k_1} \mathrm{Fe(IV)(O)(Por^{\cdot +})} + \mathrm{CH_3COO^-} \quad [1]$$

$$\mathrm{Fe(IV)(O)(Por^{\cdot +})} \xrightarrow{k_2} \mathrm{Fe(IV)(O)(Por)} \quad [2]$$

The rates of compounds I and II formation with excess PAA were monitored at isosbestic points 400 ($\varepsilon_{\text{compound I}} = \varepsilon_{\text{compound II}}$) and 415 ($\varepsilon_{\text{compound I}} = \varepsilon_{\text{Fe(III)}}$) nm, respectively (Fig. 2). Compound I formation displayed first-order kinetic profiles with fitted rate constants k_ψ. A plot of k_ψ versus [PAA] gave a second-order rate constant $k_1 = (1.28 \pm 0.04) \times 10^6\ \mathrm{M^{-1}\ s^{-1}}$. This rate is slower than that observed for HRP plus H_2O_2 ($1.7 \times 10^7\ \mathrm{M^{-1}s^{-1}}$) (14) but comparable to HRP plus ClO_2^- at its pH 4 optimum ($3 \times 10^6\ \mathrm{M^{-1}\ s^{-1}}$) (8). Compound II formation, however, is essentially independent of oxidant concentration (Figs. S6 and S7). The sigmoidal time profiles observed for compound II formation at 415 nm were fit to the biexponential rate equation:

$$[\text{Compound II}] = [\mathrm{Fe(III)}]_0\{1 - (1/(k_1[PAA] - k_2)) \cdot [k_2\exp(-k_1[PAA]t) - k_1[PAA]\exp(-k_2t)]\} \quad [3]$$

By using the value of k_1 from the second order rate plot, the data gave a first-order rate constant for Compound II formation $k_2 = 170 \pm 20\ \mathrm{s^{-1}}$ (Scheme 1). By contrast, HRP plus an equivalent of peroxide forms a compound I that persists for ≈20 min (13).

EPR of Ferryl Intermediates. The EPR spectrum of Cld in its resting state has an axial signal characteristic of high-spin ferric heme (Fig. 3). Similar spectra were observed for native chlorite dismutase from strain GR-1 and *Ideonella dechloratans*, although the latter contains an additional low-spin component not observed in our preparation (15). When the ferric enzyme was mixed with a large excess (≈4.0×10^4 eq) of chlorite and flash frozen (<1 s) in liquid N_2, the EPR signals associated with the ferric enzyme completely disappear (Fig. 3*B*). In their place, a broad S = 3/2 EPR signal characteristic of a porphyrin π-cation

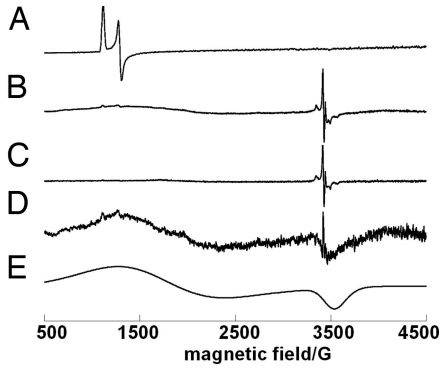

Fig. 3. EPR spectra of Cld in ferric form (*A*), during turnover with chlorite (*B*), same conditions as *B* but after warming to near the melting temperature (*C*), difference spectrum (*B* − *C*) (*D*), simulation of the axial S = 3/2 signal with $g_\perp$ = 4.5, and $g_\parallel$ = 1.99 (*E*). Concentration of enzyme and chlorite are 6.4 × 10^{-6} M and 1.0 M, respectively, in 0.010 M sodium phosphate buffer, pH 7.0. EPR spectra were recorded at 5 K.

radical (compound I) is observed, superimposed with a sharp signal at $g_\parallel$ = 2.003 and $g_\perp$ = 2.012. The g values and hyperfine pattern of the latter signal are similar to those observed for the tryptophyl radical in Ccp compound I (g = 2.037, $g_\parallel$ = 2.004), where the hyperfine is attributed to coupling to the nitrogen nuclear spin (16). On warming the sample to near the melting temperature and refreezing, the broad porphyrin π-cation radical signal disappears and the Trp radical signal grows in intensity. This is consistent with formation of compound II (EPR silent). Subtracting the EPR spectrum for the Trp radical (Fig. 3*C*) from Fig. 3*B* resulted in the spectrum of compound I porphyrin π-cation radical (Fig. 3*D*), which was simulated successfully as an axial S = 3/2 signal (Fig. 3*E*). A range of EPR signal types for compound I have been reported. The signal observed for Cld resembles that reported for compound I of ascorbate peroxidase with $g_\perp$ values at 3.3 and 1.99 (17, 18). The data are most consistent with oxidation of ferric Cld to yield compound I [Fe(IV) coupled to a porphyrin cation radical, S = 3/2]. The radical on the porphyrin is reduced by a nearby tryptophan residue, generating an EPR-silent Fe(IV)-oxo species uncoupled from the resulting EPR-active tryptophanyl radical. A strictly conserved tryptophan (Trp-189) in the immediate vicinity of the enzyme's only strictly conserved histidine (His-204) are the most likely electron donor and axial ligand, respectively.

Discussion

Cld is a heme enzyme that converts chlorite to Cl^- and dioxygen. Ion chromatography and mass spectrometry showed stoichiometric conversion of ClO_2^- to Cl^- and O_2 with no detectable oxochlorate by-products (Fig. 1; Fig. S1, Table S1). Further, even in the presence of a large excess of the appropriate diagnostic cosubstrates, dismutation is overwhelmingly favored over oxidation, halogenation, or oxygenation chemistry Table S2). This indicates that these substrates do not combine with potential reactive intermediates at the active site; nor do reactive ClO^-/HClO or ClO_2 escape from the enzyme during catalysis (Scheme S1) (8). Given the variety of known reactions catalyzed by heme and heme/chlorite systems, such specificity is extraordinary.

By contrast, in the presence of an alternate oxygen atom donor (PAA), Cld readily oxidizes one-electron peroxidase substrates (Figs. S2 and S8 and Table S2). The reaction is catalytic, with the enzyme returning to the catalytically competent, starting ferric state after each round of reaction with peracid and slightly less than 2 eq of a one-electron substrate. Thioanisole is likewise at least partially oxygenated to the corresponding sulfoxide. Unlike most peroxidases, however, Cld does not oxidize halides to the corresponding hypohaloacids (7).

Rapid-mixing UV-vis studies demonstrate the formation of compound I in the reaction of Cld with a small excess of peracetic acid (Fig. 2). This species decays in a first-order process (independent of oxidant), forming a species with the UV-vis features of compound II. The EPR spectrum for the apparent compound II generated by using chlorite resembles the tryptophanyl radical of Ccp compound I (Fig. 3), suggesting that it forms from the migration of the porphyrin radical onto a nearby tryptophan side chain. Indeed, Cld has just one strictly conserved histidine in its sequence (residue 204), which is the likely axial ligand; a strictly conserved tryptophan 15 residues upstream is a potential source of the radical. The compound II UV-vis spectrum persists for >10 s before decaying to yield a bleached heme chromophore. Rapid sequential-mixing stopped-flow experiments demonstrate that the ferric starting material is nearly completely regenerated when compound II is reacted with ascorbate (Fig. S4). The apparent compound I likewise reacts with thioanisole to partially regenerate ferric heme, compound II, and a species with a bleached UV-vis spectrum (potentially due to scission of the porphyrin macrocycle). These data indicate that Cld is *capable* of forming the expected high-valent compound I and compound II intermediates and, under rapid mixing conditions, carrying out both peroxygenase (compound I/thioanisole) and peroxidase (compound II/ascorbate) chemistry with each. The observed substoichiometric conversion of thioanisole under turnover conditions with PAA could be due to the short-lived nature of compound I (see below). In that case, the fact that peroxidase substrates are turned over in a nearly 2:1 ratio with peracid, resulting in a complete catalytic cycle, suggests that these react directly with ferryl/tryptophanyl radical pair. Alternatively, the peroxidase substrates could have better access to compound I than thioanisole or halides, possibly reacting with compound I at the heme edge (19, 20).

A mechanism for chlorite decomposition can be proposed that, by analogy, involves a compound I intermediate forming from transfer of an oxygen atom from chlorite to the ferric heme. The oxygen atoms from the resulting hypochlorite/compound I pair would subsequently recombine, in a step reminiscent of the radical rebound between substrate and heme/nonheme intermediates, to yield O_2 and Cl^-. Such a model is attractive because it is in keeping with known heme peroxidase/peroxygenase chemistry and with Cld's demonstrated ability to form high-valent, reactive intermediates with both peracid and chlorite. It is also consistent with *both* $^{18}OH_2$ and $Cl^{18}O_2^-$ labeling studies, which definitively show that the evolved O_2 originates entirely from chlorite and not from solvent water. Metalloporphyrins are known to catalyze the isomerization of peroxynitrite ($ONOO^-$), the product of the reaction between cellular superoxide and NO, to NO_3^- (21). By analogy, nucleophilic attack of ClO^- onto compound I could be envisaged to proceed via a fleeting, isomerized peroxyhypochlorite intermediate that is poised to eliminate dioxygen and chloride (Eq. **4**). This mechanism is similar to a general mechanism for O–O bond formation from metal-oxo species described by Nocera *et al.* (5), which they point out is analogous to the O–O heterolysis catalyzed by cytochrome P450s, although in reverse.

[4]

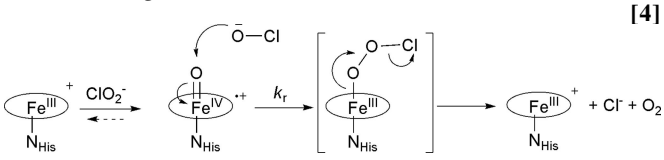

The failure to detect *any* water-derived oxygen in the evolved O_2 indicates that water and compound I do not undergo oxygen-atom exchange on the timescale of the enzymatic reaction. This

could occur if compound I were short lived (its rebound with hypochlorite is fast; cf. to oxo exchange), or if the active site were exceptionally well isolated from solvent water. The rate of conversion of compound I to compound II and its reaction rate with thioanisole (Scheme 1) are far slower than the expected rebound rates of $R^{\bullet}/HO^{\bullet}$ in cytochrome P450s and methane monooxygenase (10^9-10^{11} s^{-1}) (22). A fast recombination between the active-site-enclosed compound I/hypochlorite pair appears kinetically feasible. Based on the rate of compound II formation (k_2) and turnover number for Cld, we compute a first-order rate constant for the recombination (k_r) of $\approx 10^7$ s^{-1}. Moreover, both of these rates far exceed the rate of water/compound I oxygen-atom exchange observed for horseradish peroxidase (>1.7 s^{-1}) (23). The data are therefore consistent with the above mechanism, although decomposition of chlorite in a single, concerted step from a metal-bound chlorite cannot be ruled out. Indeed, evidence from mutation and model studies in cytochrome P450 oxidations have pointed to similar oxidant adducts as active intermediates (e.g., 24–26).

The mechanism shown in Eq. **4** is, in some ways, reminiscent of the catalase reaction. Catalases, like Cld, are most often four-subunit heme proteins, although with an axial tyrosinate ligand. Compound I forms from the reaction of ferric catalase with peroxide. This is followed by the compound I-mediated $2e^-$ oxidation of a second molecule of peroxide to generate O_2 (no new O–O bond is formed) (13). CPO, which has a cysteine-derived thiolate as its axial ligand, can also catalyze O_2 formation from H_2O_2 by a similar mechanism. This reaction is not readily catalyzed by either conventional histidine-ligated peroxidases or by Cld. CPO is moreover unique in its ability to evolve O_2 from organic peracids such as *m*CPBA. It was previously shown that the atoms in the evolved O_2 derived from two separate molecules of *m*CPBA, with compound I as an intermediate that did not undergo O atom exchange with solvent $H_2{}^{18}O$ (27, 28). Hence, the CPO/*m*CPBA reaction occurs via two sequential oxygen atom transfers in a manner remarkably similar to Eq. **4**. Although it lacks the strong electrostatic push and consequent oxidizing power supplied by the axial thiolate, Cld nonetheless formally catalyzes OAT to a substrate (ClO^-/HClO) that is itself a strong oxidant ($E'^\circ = 1.28$V, HOCl, H^+/Cl^-, H_2O at pH 7) and thermodynamically poor oxygen-atom acceptor ($E'^\circ = 1.08$V, ClO_2^-, $3H^+$/HOCl, H_2O at pH 7) (29). It apparently does so by generating the oxidizable substrate in proximity to compound I, kinetically excluding other side reactions.

Many heme oxidases and oxygenases autoinactivate in the presence of their highly oxidizing substrates (30). Chlorite dismutase was previously shown to inactivate after an extrapolated $\approx 2.0 \times 10^4$ turnovers with chlorite, concomitant with complete bleaching of the heme chromophore. Peroxidative substrates partly protect Cld from chlorite-mediated inactivation, indicating that the inactivation and peroxidase pathways share a common intermediate that is off the dismutation pathway (12); however, the reaction occurs relatively infrequently, because even a large excess of guaiacol extends Cld's turnover number only ≈10-fold. Given the mechanism shown above (Eq. **4**), this intermediate could be a ferryl/$Trp^{\bullet}$ pair, or in the event that the dismutation is concerted, compound I. Titration of the chromophore showed that Cld is far more sensitive to degradation by oxidants other than chlorite (e.g., PAA, H_2O_2, HClO). Hence, although a peroxidase-like reaction between Cld and these oxygen atom donors is possible, the enzyme is far less robust in their presence. Collectively, then, the data presented here demonstrate that chlorite dismutase is both unique among heme enzymes and exquisitely adapted for the selective detoxification of chlorite.

Methods

See *SI Text* for detailed methods and data.

Monitoring Dioxygen Evolution in Oxygen-18-Labeled Water and from Oxygen-18-Labeled Chlorite. Evolved oxygen was analyzed by using an in-house built mass spectrometer, as described in *SI Text*.

Quantitation of Cld Dismutation Products by Ion Chromatography. Chlorinated ion products were analyzed by using a Dionex DX-500 Liquid Chromatography System with a Dionex LC25 Chromatography Oven, a Dionex ED40 Electrochemical Detector, and a Dionex Ion-Pac AS9-HC ion exchange column.

Peroxidase and Halogenase Activity. The peroxidase substrates ABTS (30) and guaiacol were used in quantifying Cld-mediated $1e^-$ oxidations. Halogenase activity was monitored via disappearance of the peak at 290 nm resulting from conversion of MCD (100 μM) to dichorodimedone (DCD) ($\varepsilon = 17.7$ mM^{-1} cm^{-1}) (31) in the presence of 10 mM NaCl and 10 eq PAA or 10 mM NaBr/NaI and H_2O_2.

Screening for Cld-Mediated Oxygen Atom Transfer. Cld at 8–25 μM (heme) in a final volume of 1.5 ml was reacted under N_2 with 100 heme eq of PAA or 20,000 of chlorite in the presence of 10 mM thioanisole (sufficient oxidant to nearly quench the heme chromophore). After 1 h at 4°C (sufficient time to decompose the chlorite in the absence of thioanisole), the products were extracted with dichloromethane, condensed under N_2, resuspended in 1 ml of MeOH, and stored under N_2. Samples were analyzed by HPLC.

Stopped-Flow UV-vis Spectrophotometry. Intermediates were detected after addition of 20 eq of PAA or ClO^- to ≈10 μM Cld (in 0.1M sodium phosphate buffer, pH 7, 10°C, Applied Photophysics SX.18MV Stopped-Flow Analyzer. Thioanisole (1,500 eq) was mixed with the intermediate formed after a delay time of 10 ms (compound I) from the initial mixing of 10 μM Cld with 20 eq of PAA. For ascorbate, 600 eq were mixed with the intermediate formed after a delay time of 20 ms (compound II).

Electron Paramagnetic Resonance. Spectra were acquired on a Bruker EMX spectrometer equipped with an Oxford Instruments ITC4 helium cryostat. For Cld under turnover conditions, 75 μl of a 17 μM solution of enzyme at 4°C was placed into an EPR tube, diluted with 125 μl of a 1.7 M solution of $NaClO_2$ at 4°C, and flash frozen in liquid N_2.

UV-vis Titrations in the Presence of Oxidants. The stability of Cld in the presence of oxidants was examined by titrating Cld with increasing equivalents of PAA, H_2O_2, NaClO, or *m*CPBA. Disappearance of the heme chromophore was monitored.

ACKNOWLEDGMENTS. We thank Dr. Ekaterina V. Albert and Professor Dale W. Margerum for help with the ion chromatography experiments, and JLD thanks Garrett Moraski for helpful discussions. This work was supported by National Science Foundation Grants CHE-0502391 and CHE-0749572 (to M.M.A.-O.) and National Institutes of Health Grant ES014390-02 (to J.L.D.). B.R.S. was supported by EPA-STAR graduate fellowship FP-91690601-0.

1. Bender KS, Rice MR, Fugate WH, Coates JD, Achenbach LA (2004) Metabolic primers for detection of (Per) chlorate-reducing bacteria in the environment and phylogenetic analysis of *cld* gene sequences. *Appl Environ Microbiol* 70:5651–5658.
2. Coates JD, Achenbach LA (2004) Microbial perchlorate reduction: Rocket-fuelled metabolism. *Nat Rev Microbiol* 2:569–580.
3. Zumft WG (1997) Cell biology and molecular basis of denitrification. *Microbiol Mol Biol Rev* 61:533–616.
4. Xu JL, Song YU, Min BK, Steinberg L, Logan BE (2003) Microbial degradation of perchlorate: Principles and applications. *Environ Eng Sci* 20:405–422.
5. Betley TA, Wu Q, Van Voorhis T, Nocera DG (2008) Electronic design criteria for O-O bond formation via metal-oxo complexes. *Inorg Chem* 47:1849–1861.
6. Tagore R, Crabtree RH, Brudvig GW (2008) Oxygen evolution catalysis by a dimanganese complex and its relation to photosynthetic water oxidation. *Inorg Chem* 47:1815–1823.
7. Green MJ, Dawson JH, Gray HB (2004) Oxoiron(IV) in chloroperoxidase compound II is basic: Implications for P450 chemistry. *Science* 304:1653–1656.
8. Jakopitsch C, Spalteholz H, Fürtmuller PG, Arnhold J, Obinger C (2008) Mechanism of reaction of horseradish peroxidase with chlorite and chlorine dioxide. *J Inorg Biochem* 102:293–302.
9. Fürtmuller PG, *et al.* (2006) Active site structure and catalytic mechanisms of human peroxidases. *Arch Biochem Biophys* 445:199–213.
10. Libby RD, Thomas JA, Kaiser LW, Hager LP (1982) Chloroperoxidase halogenation reactions—Chemical versus enzymic halogenating intermediates. *J Biol Chem* 257:5030–5037.
11. Gustafsson JA, Hrycay EG, Ernster L (1976) Sodium periodate, sodium-chlorite, and organic hydroperoxides as hydroxylating agents in steroid hydroxylation reactions catalyzed by adrenocortical microsomal and mitochondrial cytochrome-P450. *Arch Biochem Biophys* 174:440–453.

12. Streit BR, DuBois JL (2008) Chemical and steady state kinetic analyses of a heterologously expressed heme dependent chlorite dismutase. *Biochemistry* 47:5271–5280.
13. Dunford HB (1999) *Heme Peroxidases* (Wiley-VCH, New York).
14. Huang LS, Wojciechowski G, Ortiz de Montellano PR (2005) Prosthetic heme modification during halide ion oxidation. Demonstration of chloride oxidation by horseradish peroxidase. *J Am Chem Soc* 127:5345–5353.
15. Stenklo K, Thorell HD, Bergius H, Aasa R, Nilsson T (2001) Chlorite dismutase from *Ideonella dechloratans*. *J Biol Inorg Chem* 6:601–607.
16. Bonagura CA, *et al.* (2003) High-resolution crystal structures and spectroscopy of native and compound I cytochrome c peroxidase. *Biochemistry* 42:5600–5608.
17. Hiner ANP, *et al.* (2001) Detection of a tryptophan radical in the reaction of ascorbate peroxidase with hydrogen peroxide. *Eur J Biochem* 268:3091–3098.
18. Patterson WR, Poulos TL, Goodin DB (1995) Identification of a porphyrin pi-cation radical in ascorbate peroxidase compound I. *Biochemistry* 34:4342–4345.
19. Ortiz de Montellano PR, Choe YS, DePillis G, Catalano CE (1987) Structure-mechanism relationships in hemoproteins. *J Biol Chem* 262:11641–11646.
20. Harris RZ, Newmyer SL, Ortiz de Montellano PR (1993) Horseradish peroxidase-catalyzed two-electron oxidations. *J Biol Chem* 268:1637–1645.
21. Szabó C, Ischiropoulos H, Radi R (2007) Peroxynitrite: Biochemistry, pathophysiology and development of therapeutics. *Nature Rev Drug Dis* 6:662–667.
22. McLain JL, Lee J, Groves JT (2000) *Biomimetic Oxidations Catalyzed by Transition Metal Complexes*, ed Meunier B (Imperial College Press, London), pp 91–169.
23. Van Haandel MJH, *et al.* (1998) Reversible formation of high-valent-iron-oxo porphyrin intermediates in heme-based catalysis: Revisiting the kinetic model for horseradish peroxidase. *Inorg Chim Acta* 275–276:98–105.
24. Collman JP, Chien AS, Eberspacher TA, Brauman JI (2000) Multiple active oxidants in cytochrome P-450 model oxidations. *J Am Chem Soc* 122:11098–11100.
25. Toy PH, Newcomb M, Coon MJ, Vaz ADN (1998) Two distinct electrophilic oxidants effect hydroxylation in cytochrome P-450-catalyzed reactions. *J Am Chem Soc* 120:9718–9719.
26. Vaz ADN, McGinnity DF, Coon MJ (1998) Epoxidation of olefins by cytochrome P450: Evidence from site-specific mutagenesis for hydroperoxo-iron as an electrophilic oxidant. *Proc Natl Acad Sci USA* 95:3555–3560.
27. Hager LP, Doubek DL, Silverstein RM, Hargis JH, Martin JC (1972) Chloroperoxidase. IX. The structure of compound I. *J Am Chem Soc* 94:4364–4366.
28. Thomas JA, Morris DR, Hager LP (1970) Chloroperoxidase VIII. Formation of peroxide and halide complexes and their relation to the mechanism of the halogenation reaction. *J Biol Chem* 245:3135–3142.
29. Arnhold J, *et al.* (2006) Kinetics and thermodynamics of halide and nitrite oxidation by mammalian heme peroxidases. *Eur J Inorg Chem* 19:3801–3811.
30. Rodriguez Lopez JN, *et al.* (1997) The inactivation and catalytic pathways of horseradish peroxidase with m-chloroperoxybenzoic acid—A spectrophotometric and transient kinetic study. *J Mol Cat A* 272:5469–5476.
31. Hewson WD, Hager LP (1979) Mechanism of the chlorination reaction catalyzed by horseradish-peroxidase with chlorite. *J Biol Chem* 254:3175–3181.